Nanoscale

PAPER

View Article Online
View Journal | View Issue

Cite this: *Nanoscale*, 2022, **14**, 14185

Investigating the role of potassium cations during electrochemical CO_2 reduction†

Sanjana Chandrashekar, *[a] Hugo-Pieter Iglesias van Montfort,[a] Divya Bohra,[a] Georgy Filonenko,[b] Hans Geerlings,[a] Thomas Burdyny[a] and Wilson A. Smith[a]

Received 22nd June 2022,
Accepted 23rd August 2022

DOI: 10.1039/d2nr03438g

rsc.li/nanoscale

The specific identity of electrolyte cations has many implications in various electrochemical reactions. However, the exact mechanism by which cations affect electrochemical reactions is not agreed upon in the literature. In this report, we investigate the role of cations during the electrochemical reduction of CO_2 by chelating the cations with cryptands, to change the interaction of the cations with the components of the electric double layer. As previously reported we do see the apparent suppression of CO_2 reduction in the absence of cations. However, using *in situ*-SEIRAS we see that CO_2 reduction does indeed take place albeit at very reduced scales. We also observe that cations play a role in tuning the absorption strengths of not only CO_2 as has been speculated, but also that of reaction products such as CO.

Electrochemical processes involve charge transfer at the electrode–electrolyte interface which aid chemical reactions such as water splitting and CO_2 reduction (ECO_2R). These interfaces play a crucial role in determining the activity and selectivity of the electrochemical reactions. Changes to the electrode composition, electrode morphology, electrolyte composition, cell architecture, *etc.*, all lead to changes in the electrode–electrolyte interface, thus affecting the reactions.

The identity of the cations used in the electrolyte during electrochemical CO_2 reduction has been shown to affect most electrochemical reactions.[1–6] Specifically, as the ionic size of the alkali cation increases, previous works have shown that ECO_2R selectivity at the cathode increases towards CO (on Au and Ag)[1] and towards C_2 products (on Cu).[4–6] In these cases, it was reported that cation with the largest ionic radius (Cs+) provided the greatest activity for ECO_2R while the smallest (Li+) provided the least enhancement. Cations accumulate at the electric double layer (EDL), due to the negatively charged cathode, with concentrations reported to be as much as ~80 times the bulk concentrations (at bulk concentrations ~0.05 M).[7–10] This condensed layer of cations at the cathode surface is important for understanding mechanisms for ECO_2R, and thus must be included in fundamental understanding and optimization of this reaction.

Many hypotheses have been put forth to describe the role of cations during ECO_2R, however a consensus still has to be reached on how cations and their hydration shells can alter the reactions taking place in the EDL. Specifically adsorbed cations are thought to have stabilizing effects on $*CO_2$ and $*COOH^-$, enabling further protonation and electrochemical reduction.[4,11,12] Cations can also change the concentration profiles of CO_2 at the electrode–electrolyte interface, and can also displace reaction intermediates to more stable reaction sites.[13–15] Another theory suggests that the cations directly affect the surface charge density and hence the interfacial electric field thus tuning the adsorption strength of reaction intermediates and also driving the concentration of CO_2 at the interface.[5,16] The key take away from these theories is that the interaction of the cations with the molecular components of the electric double layer (EDL) has a profound effect on the reaction mechanisms and thus activity and selectivity of ECO_2R.

In order to understand the exact nature of the cation's role in electrochemical processes, researchers have used chelating compounds such as crown ethers to change the interaction of the cations with the components of the EDL.[17,18] Crown ethers are 2D cyclic compounds that bind selectively to cations. Their high selectivity for cations is due to the size of their cavity matching the ionic size of the cation. However, another class of compounds called cryptands form much more stable complexes with cations compared to crown ethers. Cryptands are bi or poly-cyclic ethers that also selectively bind to cations. Their higher stability compared to crown ethers is due to their

[a]*Materials for Energy Conversion and Storage (MECS), Department of Chemical Engineering, Delft University of Technology, 2629 HZ Delft, The Netherlands. E-mail: s.chandrashekar@tudelft.nl*
[b]*Inorganic Systems Engineering (ISE), Department of Chemical Engineering, Delft University of Technology, Van der Maasweg 9, 2629 HZ Delft, The Netherlands*
† Electronic supplementary information (ESI) available. See DOI: https://doi.org/10.1039/d2nr03438g

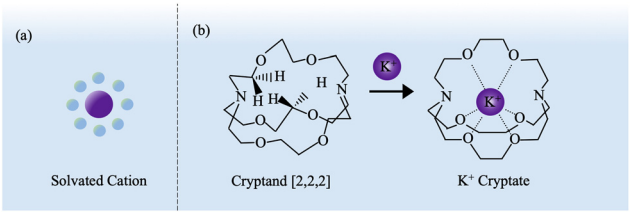

Fig. 1 Schematic representation of a potassium cation (a) chelating with Cryptand [2,2,2] to form a K^+ Cryptate (b).

3D structure that provides a more rigid structure caging in the cation, called a cryptate (Fig. 1). The complexation rate of these cryptands with the cation in an aqueous solution, compared to the rate of dissociation is much higher ($\sim 10^6$ times), indicating that in a solution with cations and cryptands, at any given moment the cryptate is the dominant component.[19]

In this report, we elucidate the role of cations in ECO_2R by changing how they interact with the reaction environment by chelating them with cryptands. The cryptands used in this report (Kryptofix [2,2,2]) bind to K^+ ions with very high selectivity and stability due to a match in the ionic size of the K^+ ion and the size of the cavity of the cryptand.[19,20] We study the effect of slowly chelating the cations in the electrolyte with cryptands, during CO_2 reduction over an Ag catalyst in an aqueous H-cell, where we observed that cations seem to be very crucial for ECO_2R to take place. Using *in situ*-surface enhanced infrared spectroscopy (SEIRAS) we find that cations directly aid in stabilizing CO_2 onto the surface of the catalyst. We also find that cations may have important interactions with other reaction intermediates and products.

To first understand the effects of chelating K^+ with cryptands, the electrochemical performance of Ag was tested by applying a constant potential in the range of −1.4 to −1.9 V (*vs.* Ag/AgCl) in an aqueous H-cell configuration (complete description of the experiments can be found in the Experimental section). The performance (current density and faradaic efficiency) of the Ag catalyst was measured with increasing concentrations of the cryptand to determine its role in driving the reaction activity and selectivity. To understand the baseline activity, the electrochemical performance of Ag was tested in a 0.1 M $KHCO_3$ electrolyte. The selectivity for CO gradually increases in this potential range, with the hydrogen evolution reaction (HER) concomitantly being suppressed (Fig. 2a). With an electrolyte of 0.05 M cryptands in 0.1 M $KHCO_3$, where a 2 : 1 ratio of K^+ to cryptands was achieved (~0.5 M K^+ concentration), the faradaic efficiency (FE) of CO decreased to <10% at all applied potentials (Fig. 2b). This sudden and large suppression of ECO_2R could indicate that the cryptates move preferentially to the catalyst surface. Chelating all the cations by using an electrolyte with the ratio of K^+ to cryptands being 1 : 1 (~0 M K^+ concentration), completely suppressed the formation of CO, while HER continued (Fig. 2c). A similar phenomenon where this complete suppression of ECO_2R in the absence of cations have been previously reported.[15,21]

Analyzing the partial current densities with no cryptands in the electrolyte, the partial current density of CO (j_{CO}) gradually increased while the partial current density of hydrogen (j_{H_2}) remained constant. When cryptands were introduced into the electrolyte and their concentration gradually increased, it was observed that the j_{CO} reduces to 0, while the j_{H_2} almost doubles at all potentials (Fig. S1†).

In order to understand the mechanism behind ECO_2R suppression and HER promotion in the presence of cryptands, SEIRAS experiments were conducted to observe the effect of the cryptates on the reaction intermediates at the catalyst surface. A cell specially designed to probe the reaction intermediates was used with Ag deposited onto a Ge crystal.[22] Experiments were conducted with a 0.1 M $KHCO_3$ electrolyte, and the cryptands concentration was slowly increased to 0.2 M (1 : 2, K^+ : cryptand, ideally 0 M K^+ concentration) by injecting

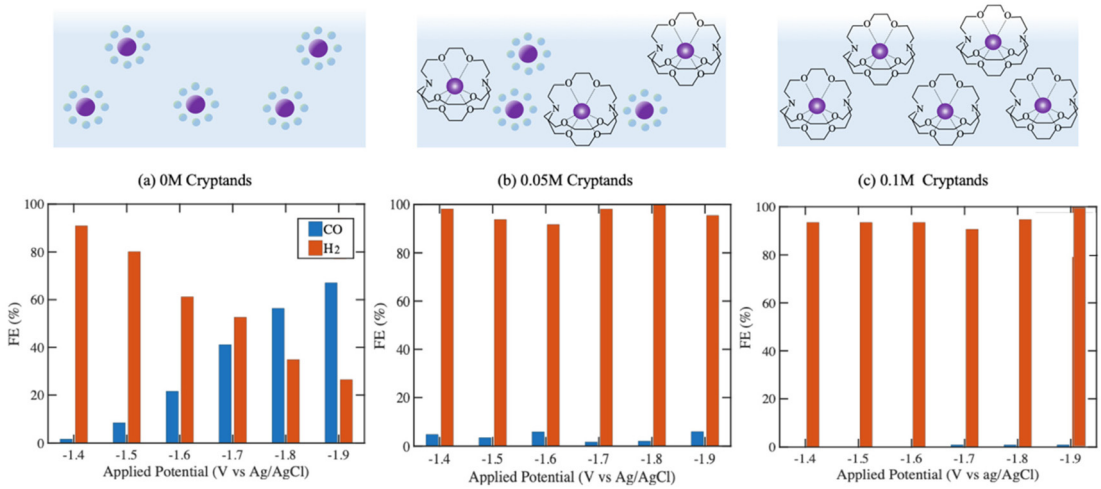

Fig. 2 Faradaic efficiencies recorded in the H-cell on an Ag catalyst deposited on Ti foil with 0.1 M $KHCO_3$ as the electrolyte, (a) with no cryptands, (b) with 0.05 M cryptands, (c) with 0.1 M cryptands.

a concentrated cryptand solution into the cell after each experiment (more details of the experiments are provided in Experimental section).

The SEIRAS spectra obtained on an activated Ag catalyst showed multiple distinct vibrational modes. Positive peaks indicate an increase in the concentration of the species whereas negative peaks indicate the depletion of certain species compared to their concentrations during the background scan. The area of these peaks give quantitative information about the species and the position of the peak center provides information on the interaction between the molecule and the catalyst surface.

The CO_2 vibrational mode was observed at ~2340 cm^{-1} as has been previously reported.[22] The peak area of CO_2 however reduces with the increasing concentration of cryptands, indicating a reduced consumption of CO_2 for ECO_2R. However, CO_2 is consumed at all concentrations of cryptands indicating that ECO_2R has surprisingly not been completely suppressed as indicated by the H-cell experiments.

Cations have been proposed to stabilize the adsorbed CO_2 molecule on to the catalyst surface enabling its conversion to various products.[12,14,16] The reduction in CO_2 peak area with increasing cryptand concentrations, suggests that lower quantities of CO_2 is being reduced to CO. This reduction in CO_2 consumption with increasing cryptand concentration, could strengthen the theory of cations stabilizing the $*CO_2$ molecule on to the catalyst. The forward scans (Fig. 3) also show that the presence of the CO_2 peak appears at more negative potentials as the cryptand concentration increases, helping to emphasize that cations do help in stabilizing CO_2 on the catalyst surface. However, the mechanism of this stabilizing effect cannot be observed in SEIRAS.

A peak corresponding to the vibrational mode of CO observed in the range of 1990–1970 cm^{-1} for the baseline experiment without cryptands, which is similar to previously reported values (Fig. 3).[22,23] As the concentration of cryptands was increased, the CO peaks did not completely vanish from the spectra, as would be expected from the H-cell results (Fig. 3). On the contrary, CO peaks were observed at all concentrations of cryptands. There is a stark difference between the CO peak area in the scans with and without cryptands (Fig. 4a), where increasing concentration of the cryptands had no noticeable effect on the area of the peak. The CO peak areas also only diverge at potentials more negative than −1.4 V *vs.* Ag/AgCl, which is the potential at which CO is detected in the H-cell experiments (Fig. 4a). The lower peak areas observed with cryptands in the electrolyte could be the result of lower concentrations of CO_2 consumed in the EDL.

The peak centers of CO shifted to lower wavenumbers at more negative potentials. This phenomena has been previously observed and can be attributed to multiple phenomena such as the increased coverage of CO molecules leading more dipole–dipole interactions and well as the Stark tuning effect.[16,22–26]

What was more evident was the shift in the peak centers of CO to lower wavenumbers (~15 cm^{-1} at −1.9 V *vs.* Ag/AgCl) as the cryptand concentration increased (Fig. 4b and c). With higher concentrations of cryptands the surface charge density induced by the cations is lowered and there exists a lower shielding of the negatively charged metal. Therefore, the metal is better equipped to support the adsorbed CO through a more effective pi-backbonding. This causes an increase in bonding strength between the catalyst and the adsorbed CO, which in turn decreases the bond length. The implications of this would lead to an increase in the bond length between the carbon and oxygen atom causing the peak centers of CO to shift to lower wavenumbers. This suggests that the CO mole-

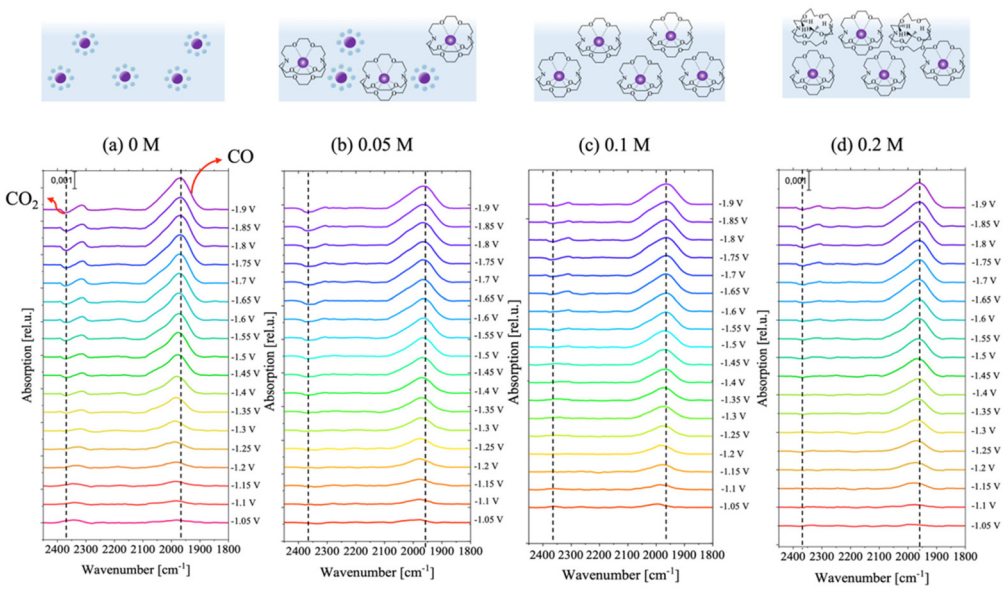

Fig. 3 *In situ* infrared spectroscopy of the electrode surface with different cryptand concentrations, showing the forward scans obtained through applied potentials −1.0 V to −1.9 V, revealing the peaks for CO_2 and CO with increasing concentrations (0 2 M to 0.2 M) of cryptands (a–d).

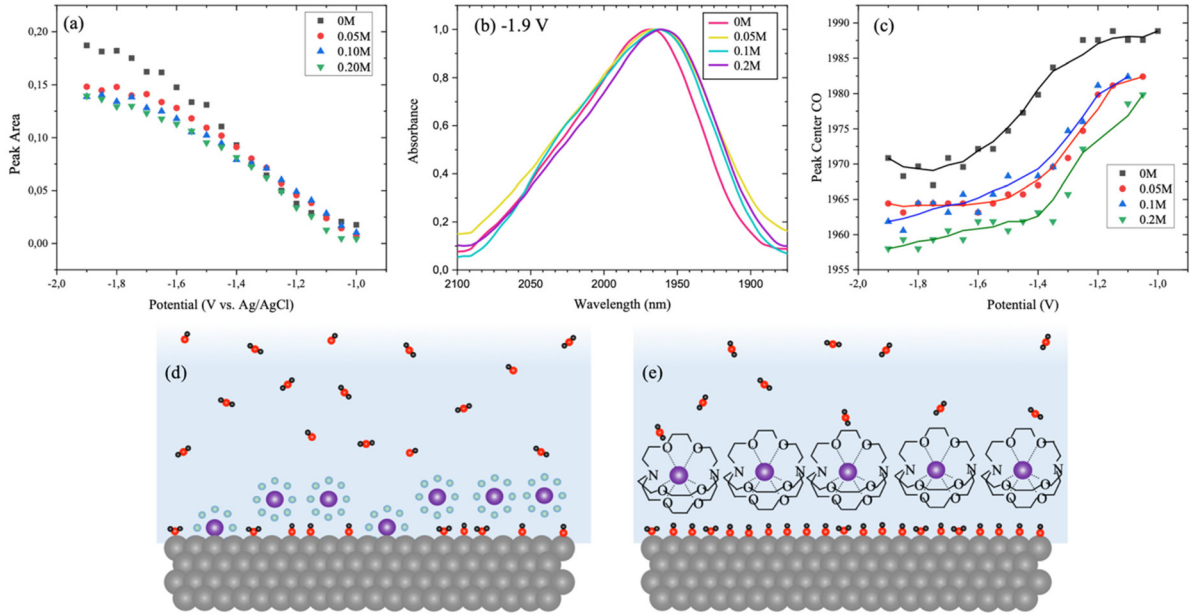

Fig. 4 Analysis of CO peak (a) CO peak areas changing with potential (b) shift in CO peak at −1.9 V at different cryptand concentrations (c) change in CO peak centers with potential at constant cryptand concentration (d) & (e) schematic representation of cations and cryptates near the catalyst surface.

cule is more strongly bound to the metal substrate in the absence of solvated K^+ cations (or by encapsulating the cations in cryptands we prevent the cations from directly interacting with the reaction intermediates and products).

To further understand the observed spectroelectrochemical trends, the difference in areas of the CO peaks with and without the cryptands was compared, finding a distinct but narrow change. In the H-cell experiments conducted using electrolytes without cryptands, CO was clearly detected with the GC. The small difference in the peak areas which indicate a small difference in the CO concentrations, implies that CO should have been detected at all concentrations of cryptands. These results thus indicate that the CO molecules remain adsorbed onto the catalyst surface in the absence of K^+ cations.

To confirm the strong adsorption of CO adsorption on the surface, the CO peak areas were monitored during the reverse (going from more negative applied potentials to less negative applied potentials) scans in the SEIRAS (Fig. S2†). These data showed that there is no discernable difference in the onset of the reduction in peak area. It was also not possible to cycle at positive potentials in order to observe CO oxidation peaks, as this would damage the catalyst layer on the Ge crystal.[22]

Furthermore, we observed a very small consumption of CO_2 (Fig. 3) in electrolytes with cryptands, but a constant increase in the peak area of CO which is disproportional to the consumption of CO_2. This could further strengthen the theory that CO concentration is increasing due to it being adsorbed on the catalyst surface and without desorbing.

In summary, we studied the effects of chelating electrolyte cations with cryptands to gain further understanding of the role of cations during the electrochemical conversion of CO_2. We report that by reducing the free cation concentrations in the electrolyte, ECO_2R appears to shut down. Using SEIRAS, we see that the absence of cations does not in fact inhibit ECO_2R, but lowers surface charge density causing the reaction products such as CO to strongly bind to the catalyst surface restricting its desorption. This lowered surface charge density also is seen to lower CO_2 consumption which can be expected from previous literature.

Experimental methods

Thin-film cathode preparation

Thin-film cathodes were deposited on 60° Ge ATR crystals (Pike Technologies, 013-3132). These crystals were polished using alumina powder suspensions of decreasing grain-size (1.0 μm, 0.3 μm and 0.05 μm) and then sonicated for 5 minutes in isopropyl alcohol and deionized water. Before mounting in the DC magnetron sputtering setup, crystals were wiped with acetone using cotton swabs. Deposition of the Ag catalyst layer was performed in a magnetron sputtering system (PEVAC Project 229), at a chamber pressure of 25 μbar, argon flowrate of 15 sccm and power rate of 25 W, for a deposition rate between 0.013 and 0.014 nm s^{-1} and thickness of 40 nm. Presence of the catalyst was confirmed both optically and by measuring the resistance over the film using a multimeter, which was between 3 and 4 Ω. This procedure is strongly based to one reported in previous literature, but avoids air- or argon-plasma cleaning of the target while delivering comparable results.[22,27]

Electrochemical SEIRAS routines

Electrochemical SEIRAS measurements were performed in a proprietary H-cell which accommodates the crystal as working

electrode. A graphite rod (Alfa Aesar, 99.9995% metals basis) served as the counter electrode, whilst the reference was a 3 M NaCl Ag/AgCl miniaturized electrode (BASI, MF-2052). The electrolyte used was 0.1 M $KHCO_3$ (Sigma-Aldrich, 99.7% ACS reagent), to which a 0.5 M cryptand (Kryptofix [222] Sigma Aldrich 99%) solution was added to achieve the target concentration.

SEIRAS spectra were collected in a Brucker Vertex 70 modified FT-IR spectrometer, averaged over 72 scans at a resolution of 4 cm^{-1}. These spectra were collected as reflectance of the signal and transformed to absorbance units (a.u.) using the relation: $A = \log(R/R_0)$. The sample chamber accommodates the proprietary cell and an additional N_2 purge. Electrochemical routines were performed using a BioLogic SP-200 potentiostat. Before any spectroscopic measurement, the cell was purged for 30 min using 99.999% pure CO_2 gas (5 sccm). This purge was also active during electrochemistry. Before starting SEIRAS experiments, the Ag thin film was activated by applying 6 cyclic voltammetries from +0.2 V to −1.1 V *vs.* Ag/AgCl. After this, background scans were collected at −0.5 V *vs.* Ag/AgCl, and consecutive scans every 50 mV during a linear sweep voltammetry at 2 mV s^{-1}. At −1.9 V, the potential was held for 7 scans before being reversed to OCV at the same scan-rate.

Electrochemical measurements

The electrochemical reduction of CO_2 was conducted in a homemade custom H-cell. The cell's body was made of Polymethyl methacrylate (PMMA) with Pt as the anode and a cation exchange membrane (Nafion NM 115 from Ion Power), separating the anode chamber from the cathode chamber. A CO_2 purge stream was constantly fed to both the anolyte and catholyte at 10 sccm each. The electrolyte used was 0.1 M $KHCO_3$ saturated with CO_2. Electrolytes with Cryptands (Kryptofix[222] Sigma Aldrich 99%) were prepared in 0.1 M $KHCO_3$ solutions and fresh electrolytes were used after every experiment. The reference electrode used was Ag/AgCl and the catholyte was constantly stirred with a magnetic stirrer to improve mass transport. Experiments were conducted by applying a constant potential (−1.4 V to −1.9 V) and measuring the current over the span of 60 minutes. The overhead gas space of the catholyte was sampled every 10 minutes by an online Gas Chromatograph (GC) (Compact GC 4.0, GAS) to determine the gaseous products formed.

Conflicts of interest

There are no conflicts to declare.

Acknowledgements

This work is part of the Advanced Research Center for Chemical Building Blocks (ARC CBBC), which is co-founded and co-financed by the Netherlands Organisation for Scientific Research (NWO) and the Netherlands Ministry of Economic Affairs. The authors of this work are also grateful to Paul Corbett, Michiel de Heer and Maarten Schellekens for their support. The authors are also grateful to the Shell Global Solutions International B.V. for their contribution. The authors are also grateful to Dr Recep Kas for helping develop much of the SEIRAS knowledge in the group.

References

1 M. R. Thorson, K. I. Siil and P. J. A. Kenis, Effect of Cations on the Electrochemical Conversion of CO2 to CO, *J. Electrochem. Soc.*, 2013, **160**(1), DOI: **10.1149/2.052301jes**.

2 C. M. Gunathunge, V. J. Ovalle and M. M. Waegele, Probing Promoting Effects of Alkali Cations on the Reduction of CO at the Aqueous Electrolyte/Copper Interface, *Phys. Chem. Chem. Phys.*, 2017, **19**(44), 30166–30172, DOI: **10.1039/c7cp06087d**.

3 O. Ayemoba and A. Cuesta, Spectroscopic Evidence of Size-Dependent Buffering of Interfacial PH by Cation Hydrolysis during CO2 Electroreduction, *ACS Appl. Mater. Interfaces*, 2017, **9**(33), 27377–27382, DOI: **10.1021/acsami.7b07351**.

4 A. Murata and Y. Hori, Product Selectivity Affected by Cationic Species in Electrochemical Reduction of CO2 and CO at a Cu Electrode, *Bull. Chem. Soc. Jpn.*, 1991, 123–127, DOI: **10.1246/bcsj.64.123**.

5 J. Resasco, L. D. Chen, E. Clark, C. Tsai, C. Hahn, T. F. Jaramillo, K. Chan and A. T. Bell, Promoter Effects of Alkali Metal Cations on the Electrochemical Reduction of Carbon Dioxide, *J. Am. Chem. Soc.*, 2017, **139**(32), DOI: **10.1021/jacs.7b06765**.

6 M. R. Singh, Y. Kwon, Y. Lum, J. W. Ager and A. T. Bell, Hydrolysis of Electrolyte Cations Enhances the Electrochemical Reduction of CO2 over Ag and Cu, *J. Am. Chem. Soc.*, 2016, **138**(39), 13006–13012, DOI: **10.1021/jacs.6b07612**.

7 S. E. Weitzner, S. A. Akhade, J. B. Varley, B. C. Wood, M. Otani, S. E. Baker and E. B. Duoss, Toward Engineering of Solution Microenvironments for the CO2Reduction Reaction: Unraveling PH and Voltage Effects from a Combined Density-Functional-Continuum Theory, *J. Phys. Chem. Lett.*, 2020, **11**(10), 4113–4118, DOI: **10.1021/acs.jpclett.0c00957**.

8 D. Bohra, J. H. Chaudhry, T. Burdyny, E. A. Pidko and W. A. Smith, Modeling the Electrical Double Layer to Understand the Reaction Environment in a CO2 Electrocatalytic System, *Energy Environ. Sci.*, 2019, **12**(11), 3380–3389, DOI: **10.1039/c9ee02485a**.

9 B. Garlyyev, S. Xue, S. Watzele, D. Scieszka and A. S. Bandarenka, Influence of the Nature of the Alkali Metal Cations on the Electrical Double-Layer Capacitance of Model Pt(111) and Au(111) Electrodes, *J. Phys. Chem. Lett.*, 2018, **9**(8), 1927–1930, DOI: **10.1021/acs.jpclett.8b00610**.

10 J. E. Huang, F. Li, A. Ozden, A. S. Rasouli, F. Pelayo, G. De Arquer, S. Liu, S. Zhang, M. Luo, Y. Xu and K. Bertens, CO_2

Electrolysis to Multi-Carbon Products in Strong Acid, *Science*, 2006, **1078**(June), 1074–1078.

11 B. Damaskin, *Weak specific adsorption of ions*, U.S.S.R., Moscow, 1975.

12 I. V. Chernyshova and S. Ponnurangam, Activation of CO 2 at the Electrode-Electrolyte Interface by a Co-Adsorbed Cation and an Electric Field, *Phys. Chem. Chem. Phys.*, 2019, **21**(17), 8797–8807, DOI: **10.1039/c8cp07807f**.

13 M. Dunwell, J. Wang, Y. Yan and B. Xu, Surface Enhanced Spectroscopic Investigations of Adsorption of Cations on Electrochemical Interfaces, *Phys. Chem. Chem. Phys.*, 2017, **19**(2), 971–975, DOI: **10.1039/c6cp07207k**.

14 L. D. Chen, M. Urushihara, K. Chan and J. K. Nørskov, Electric Field Effects in Electrochemical CO2 Reduction, *ACS Catal.*, 2016, **6**(10), 7133–7139, DOI: **10.1021/acscatal.6b02299**.

15 M. C. O. Monteiro, F. Dattila, B. Hagedoorn, R. García-muelas, N. López and M. T. M. Koper, Absence of CO2 Electroreduction on Copper, Gold and Silver Electrodes without Metal Cations in Solution. No. 100. DOI: **10.1038/s41929-021-00655-5**.

16 S. Ringe, E. L. Clark, J. Resasco, A. Walton, B. Seger, A. T. Bell and K. Chan, Understanding Cation Effects in Electrochemical CO2 Reduction, *Energy Environ. Sci.*, 2019, **12**(10), 3001–3014, DOI: **10.1039/c9ee01341e**.

17 A. G. Fink, E. W. Lees, Z. Zhang, S. Ren, R. S. Delima and C. P. Berlinguette, Impact of Alkali Cation Identity on the Conversion of HCO 3 − to CO in Bicarbonate Electrolyzers, *ChemElectroChem*, 2021, **8**(11), 2094–2100, DOI: **10.1002/celc.202100408**.

18 A. S. Malkani, J. Li, N. J. Oliveira, M. He, X. Chang, B. Xu and Q. Lu, Understanding the Electric and Nonelectric Field Components of the Cation Effect on the Electrochemical CO Reduction Reaction, *Sci. Adv.*, 2020, **6**(45), DOI: **10.1126/sciadv.abd2569**.

19 G. W. Gokel, *Chapter 3. Complexation by Crowns and Cryptands*, 2016. DOI: **10.1039/9781788010917-00064**.

20 G. Wipff and P. Auffinger, Hydration of the 222 Cryptand and 22 Cryptates Studied by Molecular Dynamics Simulations, *J. Am. Chem. Soc.*, 1991, **113**(14), 5976–5988.

21 A. N. Frumkin, Influence of Cation Adsorption on the Kinetics of Electrode Processes, *Trans. Faraday Soc.*, 1959, **55**(1), 156–167, DOI: **10.1039/tf9595500156**.

22 E. R. Corson, R. Kas, R. Kostecki, J. J. Urban, W. A. Smith, B. D. McCloskey and R. Kortlever, In Situ ATR-SEIRAS of Carbon Dioxide Reduction at a Plasmonic Silver Cathode, *J. Am. Chem. Soc.*, 2020, **142**(27), 11750–11762, DOI: **10.1021/jacs.0c01953**.

23 S. A. Shahzad, Carbon Monoxide Adsorption on Copper and Silver Electrodes during Carbon Dioxide Electroreduction Studied by Infrared Reflection Absorption Spectroscopy and Surface-Enhanced Raman Spectroscopy, *Langmuir*, 2013, **12**, 101–168, DOI: **10.1007/978-3-642-33173-2_5**.

24 M. M. Waegele, C. M. Gunathunge, J. Li and X. Li, How Cations Affect the Electric Double Layer and the Rates and Selectivity of Electrocatalytic Processes, *J. Chem. Phys.*, 2019, **151**(16), 1DUMMT, DOI: **10.1063/1.5124878**.

25 D. K. Lambert, Vibrational Stark Effect of CO on Ni(100), and CO in the Aqueous Double Layer: Experiment, Theory, and Models, *J. Chem. Phys.*, 1988, **89**(6), 3847–3860, DOI: **10.1063/1.454860**.

26 A. Görling, L. Ackermann, J. Lauber, P. Knappe and N. Rösch, On the Coadsorption of CO and Alkali Atoms at Transition Metal Surfaces: A LCGTO-LDF Cluster Study, *Surf. Sci.*, 1993, **286**(1–2), 26–45, DOI: **10.1016/0039-6028(93)90553-V**.

27 N. J. Firet and W. A. Smith, Probing the Reaction Mechanism of CO2 Electroreduction over Ag Films via Operando Infrared Spectroscopy, *ACS Catal.*, 2017, **7**(1), 606–612, DOI: **10.1021/acscatal.6b02382**.